·电子机械工程·

Study of a New Dynamic Model for Harmonic Drive in Precision Control System

LI Gang-jun[1] and CHEN Song-ming[2]

(1. Electromechanical Engineering Department, Chengdu ElectroMechanical College Chengdu 610032;
2. Press of University of Electronic Science and Technology of China Chengdu 610054)

Abstract A mathematical model of precise harmonic drives transmission system including the effects of friction and transmission flexibility is developed and identified experimentally. In our model, the characteristics of the harmonic transmission are expressed as a function, the frictions in both motor and load side are analysed, nonlinear friction is described as a function of position and velocity, the average friction is described by a second order polynomial, and the periodical part of friction is simulated by Fourier series. The consistency of simulation results and experimental outcomes confirm the effectiveness of the proposed model.

Key words friction; harmonic drive; modelling; nonlinear; precision control

精密谐波传动系统的动态模型研究

李刚俊[1]，陈松明[2]

(1. 成都电子机械高等专科学校机电系 成都 610032; 2. 电子科技大学出版社 成都 610054)

【摘要】提出了精密控制系统中谐波齿轮传动的新的数学模型，该模型综合研究了摩擦和传动挠性的影响。模型用函数描绘了谐波传动的特性，分析了谐波传动中电机一侧和载荷一侧的摩擦力，将复杂的非线性摩擦力表述为位置和速度的函数，摩擦力中的平均摩擦用二次函数表示，周期性变化的部分用傅里叶级数描述，试验数据和仿真结果的一致性证明了该模型的有效性。

关 键 词 摩擦力; 谐波传动; 建模; 非线性; 精密控制
中图分类号 TH13 **文献标识码** A doi:10.3969/j.issn.1001-0548.2010.05.020

Harmonic drive has captured more and more researcher's attention in the last decades. Because it has many advantages including near-zero backlash, high gear reduction ratio and compact design. It is more and more widely used in precision control systems. For example, in the optoelectronic automation industry, the process of attaching optical fibres to optoelectronic devices requires submicron alignment accuracy in positioning. On the other hand, the nonlinear attributes are responsible for performance degradation. Therefore, an accurate modelling of the system is critical for the use of harmonic drives, and this model should include the main nonlinear attributes of the system.

1 Introduction of Friction modelling

Friction force is proportional to load, opposes the motion, and is independent of the contact area. Now the static+Coulomb+viscous friction model is most commonly used in engineering.

So far, about thirty friction models have been presented. For small motions, a junction in static friction behaving as a spring was concluded by Dahl, then the implications for control was studied. A dynamic friction model was proposed by Ref. [1]. in 1995[1]. The model, called the LuGre model, captures

Received date: 2009 – 10 – 16; Revised date: 2010 – 08 – 06
收稿日期： 2009 – 10 – 16; 修回日期：2010 – 08 – 06
Foundation item: Supported by the Natural Science Foundation of Sichuan Province(09ZC24)
基金项目：四川省自然科学基金(09ZC24)
Biofraphy: Li Gang-jun was born in 1965. Ph.D., associate professor, his research interests include modeling of comlex systems and nonlinear control.
作者简介：李刚俊(1965 –)，男，博士，副教授，主要从事复杂系统建模与非线性控制方面的研究.

most of the friction behaviour that has been observed experimentally. This includes the Stribeck effect, hysteresis, spring-like characteristics for stiction, and varying breakaway force. The LuGre friction model is validated by the experimental results in an adaptive control scheme with friction compensation[2], and it is used to identify the friction in harmonic drives by Ref. [3] The shortcomings of the LuGre model lie in its inability to account for nonlocal memory and it cannot accommodate arbitrary displacement force transition curves[4].

In recent years, many other friction models have been proposed. Two dynamic models were applied for simulation of one-dimensional and two-dimensional stick-slip motion by Ref.[5] In the microsliding regime, a modified Coulomb friction model integrating presliding displacement was presented by Ref. [6]. Ref. [7] noticed that the friction was described only as a function of velocity in most of friction models. For harmonic drives, they proposed a new spectral-based modelling technique that described nonlinear friction as a function of position and velocity.

An overall friction model for harmonic drives was developed by Ref. [8] and a nonlinear model of harmonic drives was studied by Ref. [9] The latter model captures most nonlinear behaviours, such as kinematic error, friction, and flexibility. However, these two models do not consider the position dependent friction. The other overall model modelling all main nonlinear attributes in the harmonic drive such as kinematic error, hysteresis, and friction was proposed by Ref. [10-12]. First he observed the position dependent friction in hannonic drives, then used the Fourier series to model the position dependent friction. He also came up with a new hysteresis model for harmonic drives. In his friction model, he only considered one revolution friction on motor side, and did not observe that the friction in harmonic drives is also dependent on load side position.

2 Harmonic drives

Harmonic drives are special flexible gear transmission systems that have a nonconventional construction with teeth meshing at two diametrically opposite ends. Because of their unique construction and operation, they have many useful properties. However, these drives possess nonlinear transmission attributes that are responsible for transmission performance degradation. The main nonlinear attributes are as follows.

Kinematic error is a difference between the ideal and the actual output position. In harmonic drives, a small amplitude of periodic kinematic error exists between the ideal and the actual output position, it makes the gear ratio dependent on the input position. The error also has a dynamic component.

Flexibility is in a harmonic drive results from various compliant elements including the flexspline cup, elliptical ball bearing and gear teeth. Nonlinear interactions of the elliptical ball bearing, the flexspline, and the circular spline produce a presliding signature. Presliding is the flexible displacement in harmonic drives. In mechanical systems, presliding makes a system’s output has hysteresis attributes.

Friction is a critical problem for precision positioning. Friction in the harmonic drive, as in any other system, produces nonlinear dynamic effects, especially at slow velocities and when there is a reversal in the direction motion. The additional peculiarity of harmonic drive friction is its periodic dependence on the motor or wave generator position, and also on the load or circular spline position. The friction in a harmonic drive is very complicated and has significant influence on positioning.

3 Modelling explores

In order to study the model of harmonic drive, a set of experimental apparatus is built. A robotic manipulator with three degrees of freedom that has two arms driven by harmonic drive motors and one linear stage actuated by a timing belt driven lead screw is previously developed, and the manipulator are controled by a computer with an amplifier and an interface card. The interface card includes A/D, D/A and an encoder accessing device. Two capacitance sensors are mounted parallel to the arms of the manipulator and are used to measure the position of the arms. The overall control scheme is illustrated in Fig. 1.

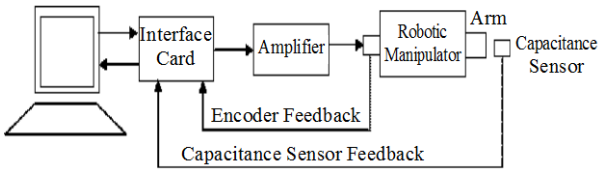

Fig. 1 Overall control scheme

3.1 Initial modelling approximations

The arms of the manipulator are driven by harmonic drive motors. Because the hysteresis effect in harmonic drives is relatively small, especially in precision impulse control, it can be negligible. A harmonic drive can be modelled as two masses connected with a spring, as shown in Fig. 2 . The control input acts on the motor and wave-generator inertia J_m, which is connected via a gear reduction r to the flexspline and arm inertia J_l. The flexibility of the harmonic drive motor plays a significant role in system dynamics and is modelled by a torsional spring that produces a torque T_s.

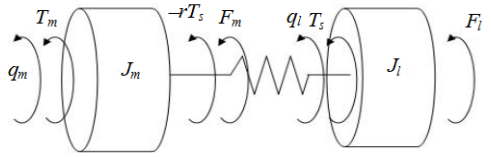

Fig. 2 Harmonic drive model

F_m and F_l stand for frictions in motor side and load side respectively in Fig. 2. Newton's second law is used for both motor and load side:

$$J_m\ddot{q}_m = T_m + F_m - T_s \tag{1}$$

$$J_l\ddot{q}_l = T_s + F_l \tag{2}$$

q_m and q_l are the positions of motor and load; T_m is the motor input torque; T_s is given by:

$$T_s = K_s(rq_m - q_l) \tag{3}$$

K_s is a spring constant of the harmonic drive.

For the armature controlled motor, motor torque can be written as:

$$T_m = K_m i_a \tag{4}$$

K_m is the motor torque constant, i_a is the armature current. It is apparent that the input voltage is:

$$u(t) = i_a R + L\frac{\mathrm{d}i_a}{\mathrm{d}t} + K_b\omega_m \tag{5}$$

where R is armature resistance, L is armature inductance, K_b is voltage constant, and ω_m is motor velocity.

From the manual, L=2.7 mH; it is very small and can be neglected. Then:

$$i_a = \frac{-K_b\dot{q}_m + u(t)}{R} \tag{6}$$

The substitution of Eg. (6) into Eg. (4) yields:

$$T_m = -\frac{K_m K_b}{R}\dot{q}_m + \frac{K_m}{R}u(t) \tag{7}$$

The substitution of Eg. (7) and Eg. (3) into Eg. (1) and Eg. (2) yields:

$$J_m\ddot{q}_m = F_m - rK_s(r\ddot{q}_m - q_l) - \frac{K_m K_b}{R}\dot{q}_m + \frac{K_m}{R}u(t) \tag{8}$$

$$J_l\ddot{q}_l = F_l + K_s(rq_m - q_l) \tag{9}$$

3.2 Friction modelling

The measurement verifies that the friction in the harmonic drive is quite position dependent, the friction varies periodically and the period is 2π, so the friction can be modelled as follows: the average of the friction can be modelled as a parabolic curve, periodical changes of friction can be modelled as a Fourier series, and the viscous effect can be modelled as a viscous coefficient multiplied by motor velocity.

The average Coulomb friction is simulated by a second order polynomial:

$$f_{\text{aver}} = s_1 q_m^2 + s_2 q_m + s_3 \tag{10}$$

By the “fminunc” function in Matlab, it is possible to minimize the Euclidian norm of error between the simulation and experimental data. The coefficients are obtained:

s_1=1.573 8e-006

s_2= –3.790 1e-004

s_3 =0.072 0

The simulation and experimental data are plotted in Fig. 3.

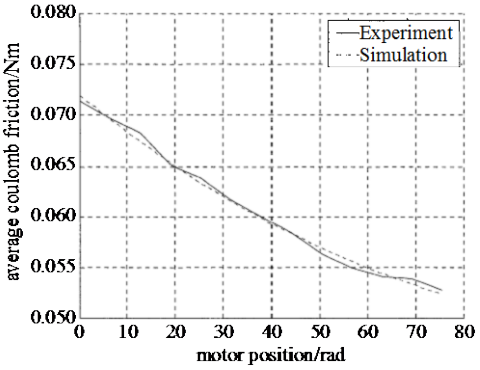

Fig. 3 Average Coulomb friction

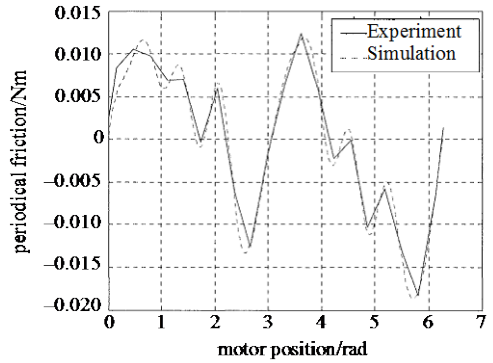

Fig. 4 Periodical friction

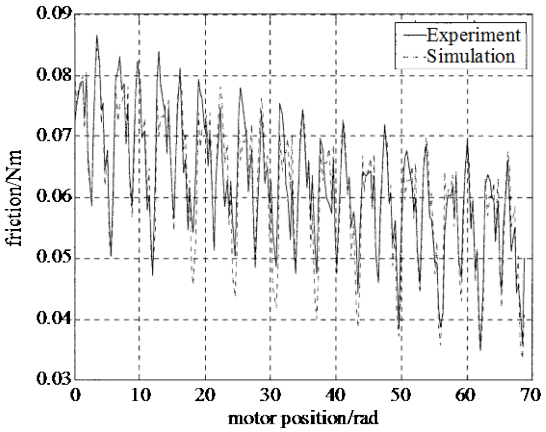

Fig. 5 Coulomb friction

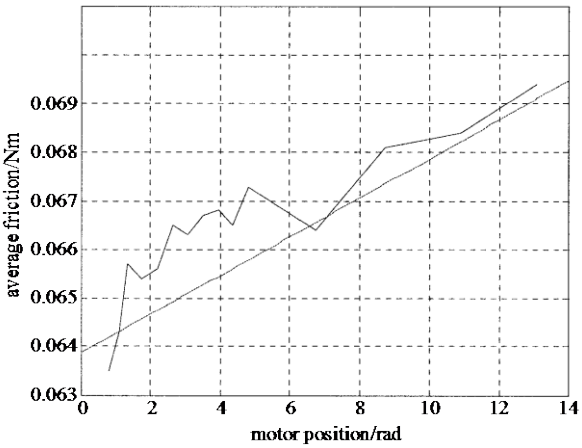

Fig. 6 Viscous friction

For the periodical term of friction, the first 2π is chosen as our simulation period. In the period of 0～2π, the average of the friction is removed from the experimental data. The friction can be expressed by a 10th order of Fourier series:

$$f_{\text{peri}} = \frac{a_0}{2} + \sum_{k=1}^{10}[a_k \cos(kq_m) + b_k \sin(kq_m)] \quad (11)$$

The Fourier coefficients (a_k, b_k) are obtained by numerical integration:

$$a_k = \frac{1}{\pi}\int_0^{2\pi} f_{\text{peri}}(q_m)\cos(kq_m)\mathrm{d}q_m \quad (12)$$

$$b_k = \frac{1}{\pi}\int_0^{2\pi} f_{\text{peri}}(q_m)\sin(kq_m)\mathrm{d}q_m \quad (13)$$

The experiment and simulation for periodical friction in the first 2π are shown in Fig. 4.

The Coulomb friction is the sum of the periodical term and average term:

$$f_{\text{coul}} = f_{\text{aver}} + f_{\text{peri}} = s_1 q_m^2 + s_2 q_m + s_3 + \frac{a_0}{2} + \sum_{k=1}^{10}[a_k \cos(kq_m) + b_k \sin(kq_m)] \quad (14)$$

The final simulation result of Coulomb friction is shown in Fig. 5. The experimental data is also plotted for comparison.

By measuring the friction in the work-range at different velocities and calculating the average value of friction, a viscous tendency can be found and it is illustrated in Fig. 6. The minimization of the Euclidian norm of error between the simulation and experimental data points is also shown in Fig. 6.

$$f_{\text{visc}} = b_m \dot{q}_m + B \quad (15)$$

The viscous coefficient b_m is 0.000 4 Nm/rad/s, B = 0.064 2.

Static friction can only be measured while the motor is moving. Therefore, only a manual measurement method can be used. Because noise exists in the system, and the kinematic error changes irregularly for different positions, static friction cannot be averaged between sampling times. In this paper, only the static friction in the first π radian range is measured. The result illustrates that there is a consistency between static and Coulomb friction. The average static friction is larger than that of Coulomb by about 3.88%. We can simply assume that the static friction is 1.038 8 times of the Coulomb friction at any position. Therefore, static friction $f_{sm}(q_m)$ can be expressed as:

$$f_{sm}(q_m) = (s_1 q_m^2 + s_2 q_m + s_3 + \frac{a_0}{2} + \sum_{k=1}^{10}[a_k \cos(kq_m) + b_k \sin(kq_m)]) \times 1.038\ 8 \quad (16)$$

3.3 Overall friction model

We can assume that the viscous coefficient is the same for different positions. This assumption is reasonable because the conditions affecting the viscous

coefficient, such as lubrication, are the same for the different positions. We also assume that the periodical friction is not velocity dependent, and the average friction varies with the velocity.

So the overall friction $f_m(q_m,\dot{q}_m)$ can be expressed by:

$$F_m=-\psi_m \quad \text{if} \quad \dot{q}_m=0,\ |\psi_m|\leqslant f_{sm}$$

$$F_m=-\text{sgn}(\psi_m)f_{sm} \quad \text{if} \quad \dot{q}_m=0,\ |\psi_m|>f_{sm}$$

$$F_m=(s_1q_m^2+s_2q_m+s_3)\times((\dot{q}_m-Vc)\times 0.0004+1)+$$

$$\frac{a_0}{2}+\sum_{k=1}^{10}[a_k\cos(kq_m)+b_k\sin(kq_m)]) \quad \text{if} \quad |\dot{q}_m|>0 \quad (17)$$

where:

$$\psi_m=-rK_s(rq_m-q_l)+\frac{K_m}{R}u(t)$$

ψ_m is input torque when $\dot{q}_m=0$, f_{sm} is calculated in Eq. (16), and V_c=0.8 rad/s stands for the motor side velocity of Coulomb friction.

3.4 Average friction model

The measured friction is quite position dependent. In our precision impulse control, the control range is small, and static friction and Coulomb friction can be averaged and considered constants. The friction used in Eqs. (8) and (9) can be modelled as static + viscous + coulomb. Thís model is accurate enough for most engineering applications. The motor side and load side frictíon can be written as:

$$F_m=-\psi_m \quad \text{if} \quad \dot{q}_m=0,\ |\psi_m|\leqslant f_{sm}$$

$$F_m=-\text{sgn}(\psi_m)f_{sm} \quad \text{if} \quad \dot{q}_m=0,\quad |\psi_m|>f_{sm}$$

$$F_m=-\text{sgn}(\dot{q}_m)f_{cm}-b_m\dot{q}_m \quad \text{if} \quad |\dot{q}_m|>0$$

$$\psi_m=-rK_s(rq_m-q_l)+\frac{K_m}{R}u(t) \quad (18)$$

and

$$F_l=-\psi_l \quad \text{if} \quad \dot{q}_l=0,\ |\psi_l|\leqslant f_{sl}$$

$$F_l=-\text{sgn}(\psi_l)f_{sl} \quad \text{if} \quad \dot{q}_l=0,\ |\psi_l|>f_{sl}$$

$$F_l=-\text{sgn}(\dot{q}_l)f_{cl}-b_l\dot{q}_l \quad \text{if} \quad |\dot{q}_l|>0$$

$$\psi_l=K_s(rq_m-q_l) \quad (19)$$

ψ_l is the spring torque when $\dot{q}_l=0$, f_{sm} and f_{cm} are motor side static friction and Coulomb friction. f_{sl} and f_{cl} are load side static friction and Coulomb friction.

3.5 State equations

We define the state variables as:

$$\begin{bmatrix}x_1\\x_2\\x_3\\x_4\end{bmatrix}=\begin{bmatrix}q_m\\\dot{q}_m\\q_l\\\dot{q}_l\end{bmatrix} \quad (20)$$

Then, the Eqs. (8) and (9) can be written in state variable format:

$$\begin{bmatrix}\dot{x}_1\\\dot{x}_2\\\dot{x}_3\\\dot{x}_4\end{bmatrix}=\begin{bmatrix}x_2\\\frac{F_m}{J_m}-\frac{rK_s}{J_m}(rx_1-x_3)-\frac{K_mK_b}{J_mR}x_2+\frac{K_m}{J_mR}u(t)\\x_4\\\frac{F_l}{J_l}+\frac{K_s}{J_l}(rx_1-x_3)\end{bmatrix} \quad (21)$$

4 Conclusion

In this paper, a mathematical model of harmonic drives in precision control system has been developed. The main nonlinear attributes of harmonic drives are analysed. A function of position and velocity is used to describe nonlinear friction. Experiments and simulation results validate and the model, the control response of harmonic transmission can predicted accurately by the model. It will be facilitate the development and applications of control method for harmonic drives.

References

[1] CARLOS C W, OLSSON H, ASTROM K J, et al. A new model for control of systems with friction[J]. IEEE Transaction Automatic Control, 1995, 40(3): 419-425.

[2] CARLOS C W, LISCHINSKY P. Adaptive friction compensation with partially known dynamic friction model[J]. Intenational Journal of Adaptive Control and Signal Processing, 1997, 11(1): 65-80.

[3] GANDHI P S, GHORBEL F H, DABNEY J. Modelling, identification, and compensation of friction in harmonic drives[C]//Proc of 41st IEEE Conf on Decision and Control. Las Vegas: [s.n.], 2002: 160-166.

[4] MARTON L, LANTOS B. Modeling, identification, and compensation of stick-slip friction[J]. IEEE Transaction Industry Electronics, 2007, 54(1): 511-521.

[5] TARIKU F A, ROGERS R J. Improved dynamic friction models for simulation of one-dimensional and two-dimensional stick-slip motion[J]. Journal of Tribology, 2001, 123(10): 661-669.

[6] WU R H, TUNG P C. Studies of stick-slip friction, presliding displacement, and hunting[J]. J of Dynamic systems, measurement, and control, 2002, 124(3): 111-117.

(下转第773页)

Transactions on Signal Processing, 2003, 51(7): 1995-2007.
[6] 张 涛, 平西建. 空域LSB信息伪装的隐写分析及其对策[J]. 通信学报, 2003, 24(12): 156-163.
ZHANG Tao, PING Xi-jian. Steganalysis of spatial LSB-based steganographic algorithms and countermeasures [J]. Journal of China Institute of Communications, 2003, 24(12): 156-163.
[7] 罗向阳, 陆佩忠, 刘粉林. 一类可抵御SPA分析的动态补偿LSB信息隐藏方法[J]. 计算机学报, 2007, 30(3): 463 - 473.
LUO Xiang-yang, LU Pei-zhong, LIU Fen-lin. A dynamic compensation LSB steganography method defeating SPA[J]. Chinese Journal of Computers, 2007, 30(3): 463-473.
[8] LUO Xiang-yang, HU Zong-yun, YANG Can, et al. A secure LSB steganography system defeating sample pair analysis based on chaos system and dynamic compensation[C]// Advanced Communication Technology on the 8th International Conference. Phoenix Park: [s.n.], 2006.
[9] 田 源, 程义民, 谢于明, 等. 一种抗SPA分析的图像信息隐藏方法[J]. 中国科学技术大学学报, 2008, 38(12): 1376-1380.
TIAN Yuan, CHENG Yi-min, XIE Yu-ming, et al. Steganographic scheme for images against SPA steganalysis [J]. Journal of University of Science and Technology of China, 2008, 38(12): 1376-1380.
[10] 汪小帆, 戴跃伟, 茅耀斌. 信息隐藏技术-方法与应用[M]. 北京: 机械工业出版社, 2001: 124-125.
WANG Xiao-fan, DAN Yue-wei, MAO Yao-bin[M]. Information Hiding Technology-Methods and application. Beijing: China Machine Press, 2001: 124-125.
[11] WANG Hong, PENG Jian-hua, ZHOU Zheng-ou. Design of a new chaos circuit and its encryption to digital information[J]. Journal of Electronic Science and Technology of China, 2004, 2(4): 25-28.

编 辑 蒋 晓

(上接第746页)

[7] POPOVIC M R, GOLDENBERG A A. Modelling of friction using spectral analysis[J]. IEEE Transaction on Robotics and Automation, 1998, 14(1): 114-122.
[8] TAGHIRAD H D, BELANGER P R. Model1ing and parameter identification of harmonic drive systems[J]. J of Dynamic Systems, Measurement, and Control, 1998, 120(6): 439-444.
[9] TUTTLE T D, SEERING W P. A Nonlinear Model of a Harmonic Drive Gear Transmission[J]. IEEE Transaction on Robotics and Automation, 1996, 12(3): 368-374.
[10] LEMMER L, KISS B. Modeling, identification, and control of harmonic drives for mobile vehicles[C]// Proceedings of the IEEE 3rd International Conference on Mechatronics. Budapest: IEEE Press, 2006: 369-374.
[11] CHOI J J, HAN S I, KIM J S. Development of a novel dynamic friction model and precise tracking control using adaptive back-stepping sliding mode controller[J]. Mechatronics, 2006, 16(2): 97-104.
[12] JATTA F, LEGNANI G, VISIOLI, A. Friction compensation in hybrid force/velocity control of industrial manipulators[J]. IEEE Transaction Industry Electronics, 2006, 53(2): 604-613.

编 辑 张 俊

(上接第761页)

[14] 田 宏, 董爱杰. 基于向量矩阵的频繁项集挖掘算法[J]. 大连交通大学学报, 2008, 29(3): 74-77.
TIAN Hong, DONG Ai-jie. A frequent itemsets mining algorithm based on vector matrix[J]. Journal of Dalian Jiaotong University, 2008, 29(3): 74-77.
[15] 张忠平, 李 岩, 杨 静. 基于矩阵的频繁项集挖掘算法[J]. 计算机工程, 2009, 35(1): 84-86.
ZHANG Zhong-ping, LI Yan, YANG Jing. Frequent itemsets mining algorithm based on matrix[J]. Computer Engineering, 2009, 35(1): 84-86.

编 辑 漆 蓉